



# Score-based free-form architectures for high-dimensional Fokker-Planck equations

**Feng Liu**<sup>1,3,4,5</sup>   **Faguo Wu**<sup>1,4,5,6,\*</sup>   **Xiao Zhang**<sup>2,4,5,6,7,\*</sup>

<sup>1</sup> School of Artificial Intelligence, Beihang University

<sup>2</sup> School of Mathematical Sciences, Beihang University

<sup>3</sup> National Superior College for Engineers, Beihang University

<sup>4</sup> Key Laboratory of Mathematics, Informatics and Behavioral Semantics, Ministry of Education

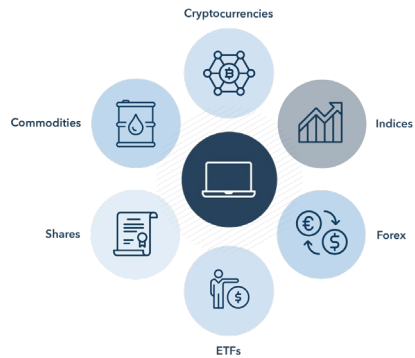
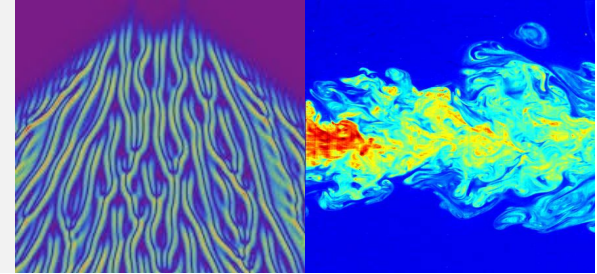
<sup>5</sup> Zhongguancun Laboratory

<sup>6</sup> Beijing Advanced Innovation Center for Future Blockchain and Privacy Computing

<sup>7</sup> Hangzhou International Innovation Institute, Beihang University

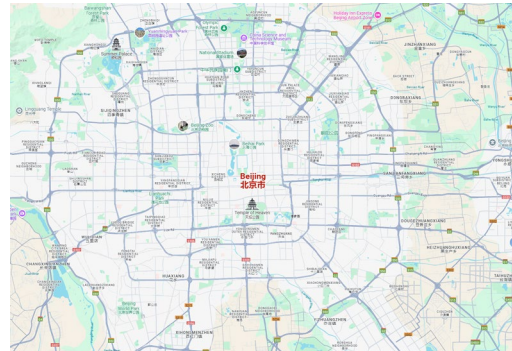
## Stochastic Dynamical Systems

**The Fokker–Planck equation** governs the time-varying probability density of dynamical systems driven by stochastic processes, with applications in statistical physics, finance, traffic flow prediction, epidemic spread simulation and climate modeling.



### Stock Market

Governs stochastic processes in stock price movements, depicting risk modeling and option pricing.



### Traffic Flow Prediction

Describes how cars or pedestrians move under uncertainty, helping optimize urban mobility.



### Epidemic Spread

Simulates how diseases spread in populations with random interactions, aiding pandemic modeling.



### Climate Modeling

Helps study stochastic climate variability, often represented in weather and ocean current simulations.

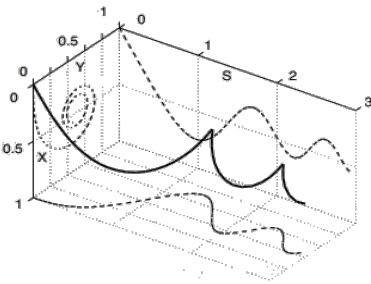
## Fokker-Planck Equations and Challenges

- Stochastic differential equation:  $dx = \mu(x, t)dt + \sigma(x, t)dW_t$
- Steady-state FP equation:

$$\frac{\partial p(x)}{\partial t} = \mathcal{L}p := - \sum_{i=1}^d \frac{\partial(p\mu_i)}{\partial x_i} + \sum_{i=1}^d \sum_{j=1}^d \frac{\partial^2(D_{i,j}p)}{\partial x_i \partial x_j} = -\nabla \cdot (p\mu) + \nabla \cdot [\nabla \cdot (Dp)]$$

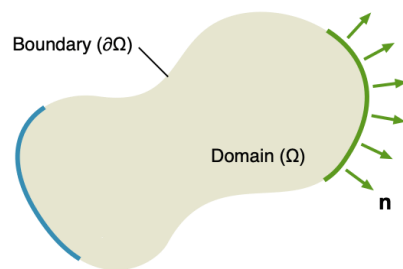
*i.e.*

$$\mathcal{L}p(x) = 0, \quad x \in \mathbb{R}^d$$



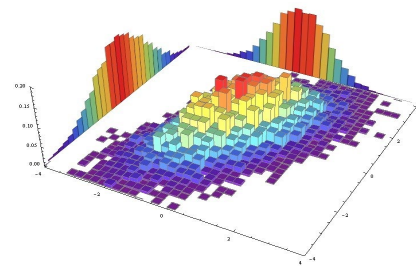
High-dimensional variables

$$p(x) \rightarrow 0, \quad (\|x\| \rightarrow \infty)$$



Unbounded spatial domains

$$\int_{\mathbb{R}^d} p(x) dx = 1$$



Normalization condition

## Physics-informed Neural Networks

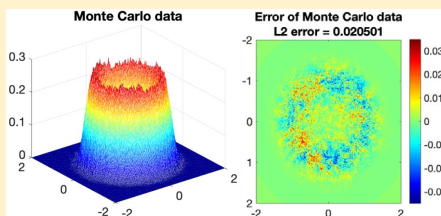
- Plain PDE loss:  $\mathcal{J}_{\text{plain}}(p_\theta) = \mathbb{E}_{x \sim U(\Omega)} \left[ \left| -\nabla \cdot (p_\theta(x) \mu(x)) + \nabla \cdot (\nabla \cdot (D(x) p_\theta(x))) \right|^2 \right]$
- Both  $p$  and  $Zp$  satisfy the SFP equation:  $\mathcal{L}p = 0$
- Directly minimizing  $\mathcal{J}_{\text{plain}}$  makes  $p_\theta \approx Zp$  converge to a trivial solution.

## Deep learning methods

### Data Driven

Labeled data:  $\{(x_j, p_j)\}_{j=1}^N$

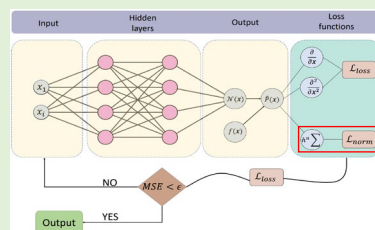
$$\mathcal{J}_{\text{label}}(p_\theta) = \frac{1}{N} \sum_{j=1}^N (p_\theta(x_j) - p_j)^2$$



### Normalization Condition

Soft Constraints.

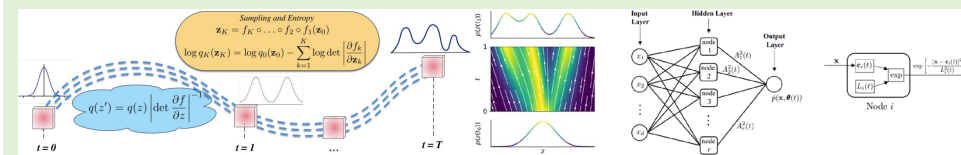
$$\mathcal{J}_{\text{norm}}(p_\theta) = \left( \frac{\nu(\Omega)}{|\mathcal{D}|} \sum_{x \in \mathcal{D}} p_\theta(x) - 1 \right)^2$$



Hard Constraints.

- Normalizing Flows:  $p_X(x) = p_Z(z) |\det \nabla_x f(x)|$
- Shape-morphing Gaussians:

$$p(x; \theta(t)) = \sum_{i=1}^r A_i^2(t) \exp \left[ -\frac{|x - c_i(t)|^2}{L_i^2(t)} \right]$$



## Limitations

- **Data-driven:** few labels, low accuracy, computational burden.
- **Normalization:** trade-offs between representation capabilities and normalization constraints.

### Model and Constraints

- **Soft constraints** often **violate the physical laws**.
- **Hard constraints** may **sacrifice the representation capacity**.

### Optimize dynamics

- $\mathcal{J}_{\text{plain}}$  tends to push the solution to zero.
- $\mathcal{J}_{\text{norm}}$  prevents the zero solution on domain.
- These **conflicting forces** result in a **tortuous optimization process** that often requires delicate manual balancing.

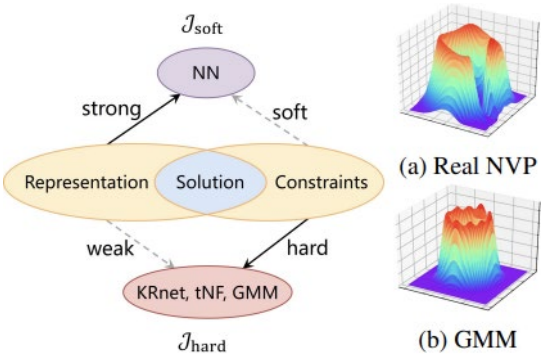


Table 1: Deep learning methods for SFP equations.

Methods	Loss function	Model	Arbitrary NN?	Whether strictly satisfy NC?
Data-Driven	$\mathcal{J}_{\text{plain}} + \lambda \mathcal{J}_{\text{label}}$	$p_{\theta}(\mathbf{x}) = p_{\text{NN}}(\mathbf{x}; \theta)$	✓	✗
Normalization Condition	$\mathcal{J}_{\text{plain}} + \lambda \mathcal{J}_{\text{norm}}$	$p_{\theta}(\mathbf{x}) = p_{\text{NN}}(\mathbf{x}; \theta)$	✓	✗
	$\mathcal{J}_{\text{plain}}(p_{\theta})$	$p_{\theta}(\mathbf{x}) = p_{\text{KRnet}}(\mathbf{x}; \theta), p_{\text{GMM}}(\mathbf{x}; \theta), p_{\text{TN}}(\mathbf{x}; \theta) \cdots$	✗	✓
	$\mathcal{J}_{\text{score}}(\tilde{p}_{\theta})$	$\tilde{p}_{\theta}(\mathbf{x}) = \tilde{p}_{\text{NN}}(\mathbf{x}; \theta), p_{\theta}(\mathbf{x}) = \frac{\tilde{p}_{\theta}(\mathbf{x})}{\int \tilde{p}_{\theta}(\mathbf{y}) d\mathbf{y}}$	✓	✓

## Fokker-Planck Neural Network

- We propose a Fokker-Planck neural network (FPNN) framework to efficiently solve high-dimensional SFP equations, decoupling **the score learning** and **the density normalization** into two stages.
- **Stein Score**  $\nabla_x \log p$ :  $p_\theta(\mathbf{x}) = \frac{\tilde{p}_\theta(\mathbf{x})}{Z_\theta}$ ,  $Z_\theta = \int \tilde{p}_\theta(\mathbf{x}) d\mathbf{x}$   $\log p_\theta(\mathbf{x}) = \log \tilde{p}_\theta(\mathbf{x}) - \log Z_\theta$   $\nabla \log p_\theta(\mathbf{x}) = \nabla \log \tilde{p}_\theta(\mathbf{x})$
- **Key idea:** Since  $p_\theta$  and  $\tilde{p}_\theta$  share the same score, we can derive a score PDE loss of SFP equations to bypass the normalization condition.
- **Derivation of Score PDE Loss:**

$$\begin{aligned}\mathcal{L}p(x) &= -\nabla \cdot (p\mu) + \nabla \cdot \nabla \cdot (Dp) \\ &= -\nabla \cdot (p\mu - (\nabla \cdot D)p - D\nabla p) \\ &= -\nabla \cdot (p(\mu - \nabla \cdot D - D\nabla \log p)) \\ &= -\nabla \cdot (p\tilde{\mu})\end{aligned}$$

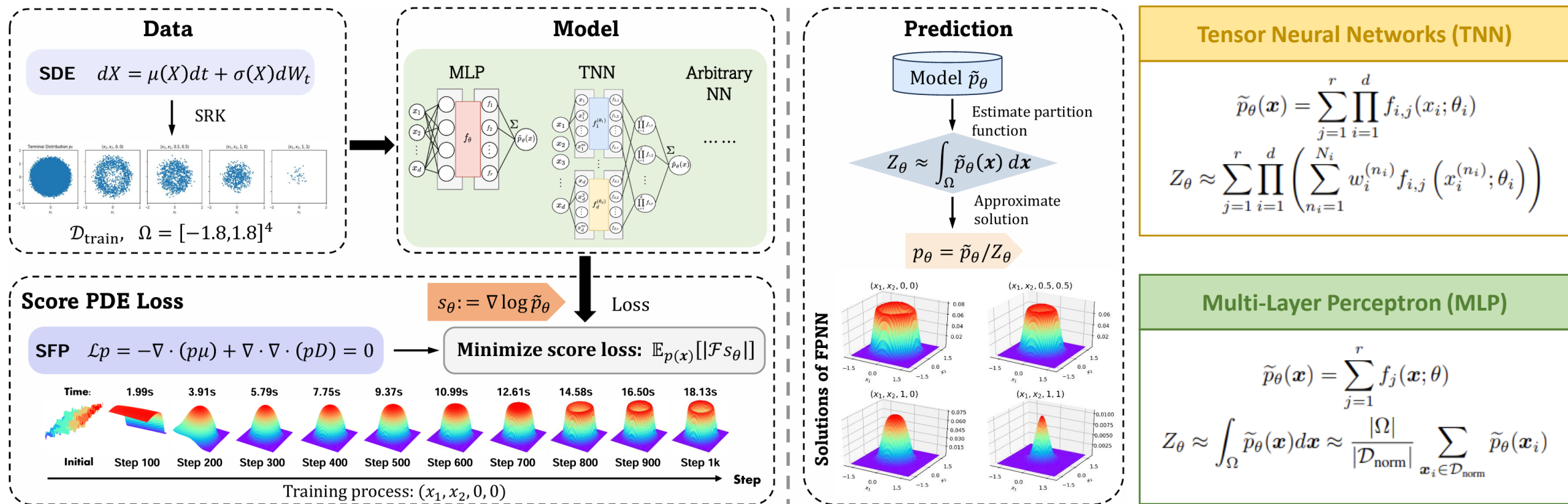
$$\tilde{\mu} := \mu - \nabla \cdot D - D\nabla \log p$$

$$\begin{aligned}\mathcal{J}_{\text{plain}}(p_\theta) &= \mathbb{E}_{q(x)}[|\mathcal{L}p_\theta(x)|] = \int_{\Omega} \frac{1}{v(\Omega)} |\mathcal{L}p_\theta(x)| dx \\ &= \frac{1}{v(\Omega)} \int_{\Omega} |\nabla p_\theta \cdot \tilde{\mu} + p_\theta(\nabla \cdot \tilde{\mu})| dx \\ &= \frac{1}{v(\Omega)} \mathbb{E}_{p_\theta(x)}[|\nabla \log p_\theta \cdot \tilde{\mu} + (\nabla \cdot \tilde{\mu})|] \\ &\approx \frac{1}{v(\Omega)} \mathbb{E}_{p(x)}[|\mathcal{F}s_\theta(x)|] = \frac{1}{v(\Omega)} \mathcal{J}_{\text{score}}(s_\theta)\end{aligned}$$



## Framework

- Score PDE Loss:**  $\mathbb{E}_{p(x)}[|\mathcal{F}s_\theta(x)|] := \mathbb{E}_{x \sim p(x)}[|s_\theta(x) \cdot \tilde{\mu}(x) + \nabla \cdot \tilde{\mu}(x)|]$   
 $\tilde{\mu}(x) := \mu(x) - \nabla \cdot D(x) - D(x)s_\theta(x)$



## Accuracy

- **TFFN** can not learn the solution correctly with **50,688** parameters and 20k steps in 6D Unimodal problem.
- **FPNN** gets average relative errors of **11.36%**, **13.87%** and **12.72%** for 4D Ring, 6D Unimodal and 6D Multi-modal problems respectively, requiring only **256**, **980**, and **980** parameters.

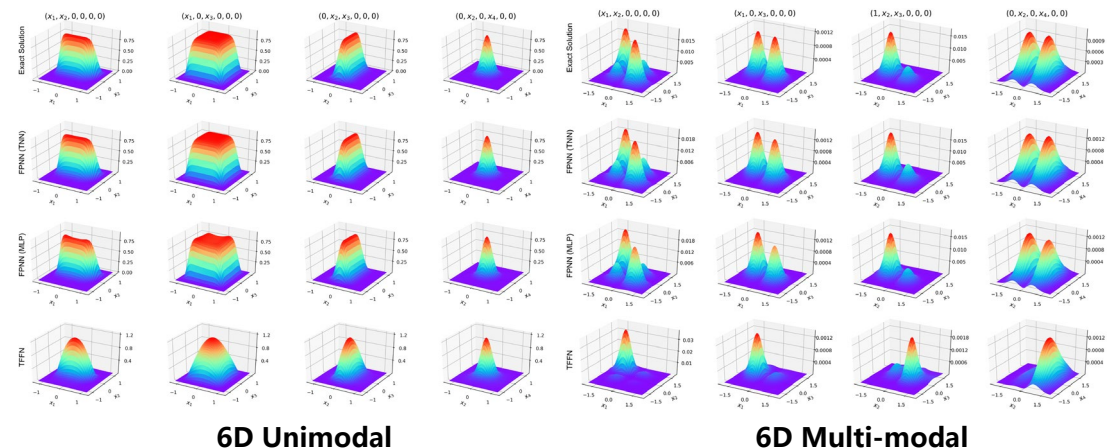
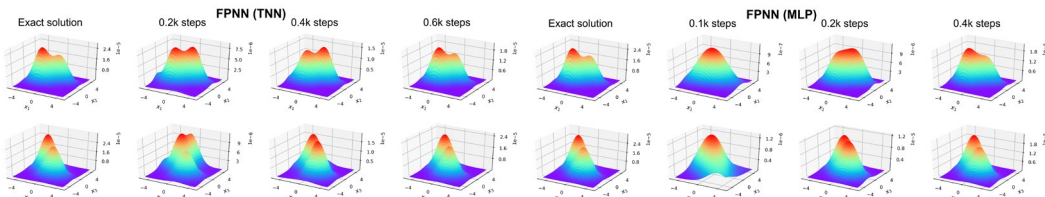
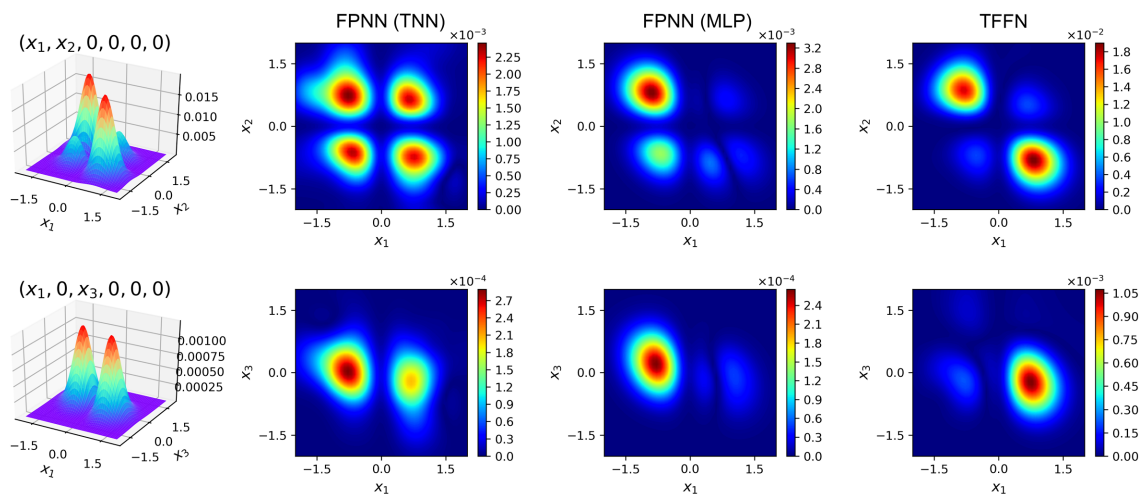


Table 2: Experimental results of TFFN and FPNN on 4-6 dimensional SFP equations.

SFP equations	Domain $\Omega$	TFFN		FPNN (Ours)	
		MAE	MAPE	MAE	MAPE
4D Ring	$[-1.8, 1.8]^4$	$3.61 \times 10^{-3}$	49.25%	$5.56 \times 10^{-4}$	3.84%
6D Unimodal	$[-1.2, 1.2]^6$	$4.00 \times 10^{-2}$	293%	$1.48 \times 10^{-3}$	4.33%
6D Multi-modal	$[-2, 2]^6$	$1.84 \times 10^{-3}$	92.90%	$1.98 \times 10^{-4}$	12.18%



10D Gaussian mixture: predicted solutions

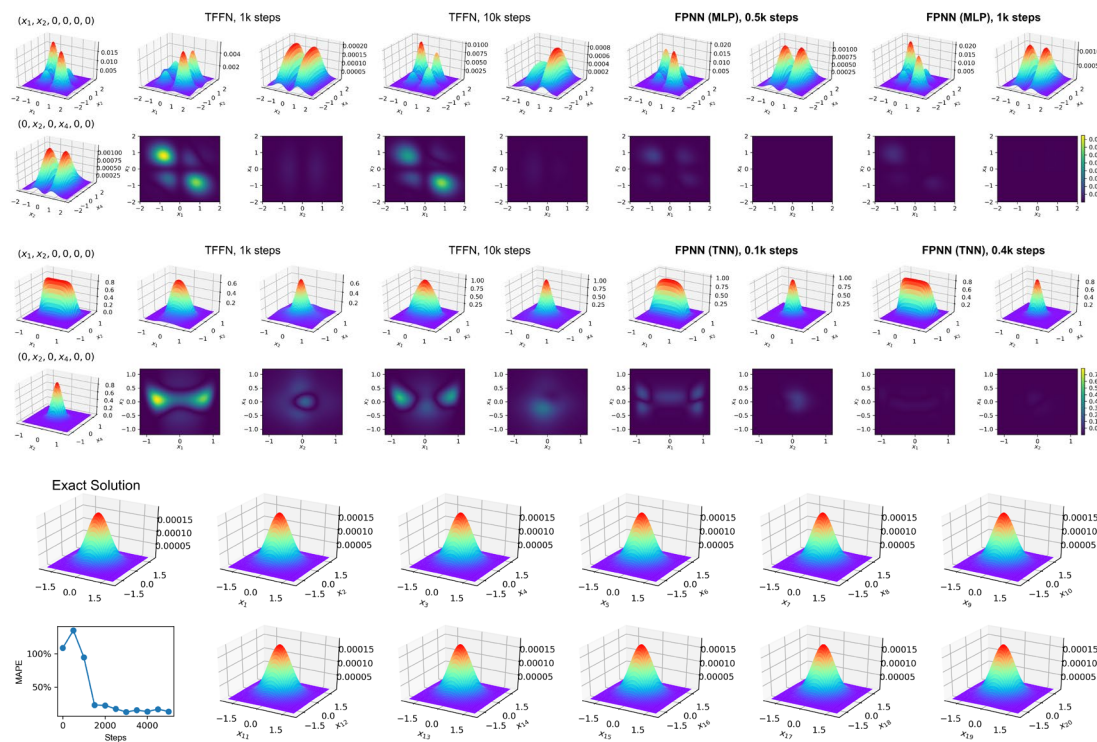


6D Multi-modal: absolute errors

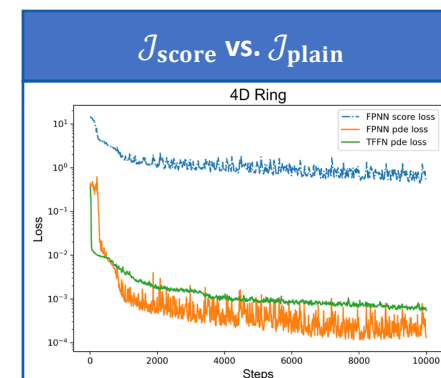
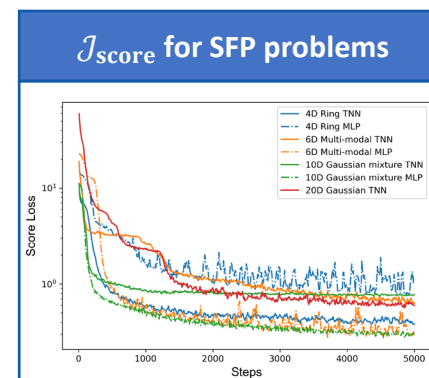


## Efficiency

- FPNN successfully learn the multi-modal at **1k** steps, and capture the 6-dimensional peak in **400** steps. Score PDE loss makes the training dynamics more coherent and efficient, so we solve SFP equations much faster than TFFN.



20D Gaussian: predicted solutions



Model	Layers	Parameters	MAE	MAPE
TNN	[ $m$ , hidden layers, $r$ ]			
	[1, 64, 128]	33,792	$7.27 \times 10^{-3}$	99.82%
	[3, 20, 20, 20, 20]	5,360	$4.25 \times 10^{-3}$	65.41%
	[3, 64, 64, 64]	34,304	$6.91 \times 10^{-4}$	7.58%
	[5, 64, 128]	34,816	$8.20 \times 10^{-4}$	5.66%
MLP	[8, 64, 128]	35,584	$5.56 \times 10^{-4}$	3.84%
	[ $d$ , hidden layers]			
	[4, 8, 8, 8, 8]	256	$1.26 \times 10^{-3}$	11.36%
	[4, 20, 20, 20, 20]	1,360	$9.74 \times 10^{-4}$	8.74%
	[4, 64, 64, 64]	8,640	$8.81 \times 10^{-4}$	6.48%
	[4, 128, 128]	17,152	$6.21 \times 10^{-4}$	5.39%

4D Ring: FPNN with different networks

- We successfully solve **4-20** dimensional steady-state FP equations for complex physical systems and comprehensive experimental results show great gains in **efficiency**, **accuracy**, **memory** and **computational resource usage**.
- **Time-varying** probability densities have broader applications in physics, finance, mean-field games, and diffusion models, but still face challenges for the normalization condition at any time.
- In the future, we aim to develop an efficient deep-learning solver for general Fokker-Planck equations and look forward to its applications in broader fields.



**ICLR**  
International Conference On  
Learning Representations



**北京航空航天大学**  
BEIHANG UNIVERSITY

# Thank you!

**Paper:** <https://openreview.net/forum?id=5qg6JPSgCj>

**Code:** <https://github.com/niuffs/FPNN>

